

Pressure-Dependent Photon Correlation Spectroscopic Investigation of Poly(propylene oxide) near the Glass Transition

Steven W. Smith,[†] Benny D. Freeman,* and Carol K. Hall

Department of Chemical Engineering, North Carolina State University,
Raleigh, North Carolina 27695-7905

Received March 19, 1996; Revised Manuscript Received December 27, 1996[®]

ABSTRACT: The effect of pressure on structural relaxations in poly(propylene oxide) (PPO; MW = 4000) near the glass transition has been determined using photon correlation spectroscopy. Experimental results are reported for pressures ranging from 2.5 to 3.9 kbar at 253 K. The structural relaxation exhibits two distinct processes separated by ~ 3 orders of magnitude in time. This observation is consistent with results of dielectric relaxation studies of PPO. The faster relaxation is associated with local segmental motions important in the glass–rubber transition. The mean relaxation time for the faster process exhibits an exponential dependence on pressure.

Introduction

The importance of the glass–rubber transition and its impact on polymer mechanical properties has prompted the development of numerous methods for its characterization. In polymers, structural relaxations near the glass–rubber transition decay nonexponentially over many decades in time and can be characterized by dielectric and nuclear magnetic relaxation, neutron and light scattering, and mechanical spectroscopy experiments.¹ As the temperature of a rubbery polymer decreases (or as pressure increases), the fractional free volume decreases and the molecular motion is slowed to the point where localized segmental motions begin to play the dominant role in structural relaxation. A molecular-level description of the motions responsible for structural relaxations near the glass transition remains elusive because experiments do not monitor molecular motions directly but, instead, probe their corresponding footprints such as dipole moment, dielectric tensor, stress, or strain. Despite the absence of a complete molecular-level description for structural relaxations, its nonexponential character is commonly attributed to either (1) a distribution of independent exponential relaxations or (2) a hierarchy of dynamic constraints which couple segmental (short-range) and molecular (long-range) motions.²

Photon correlation spectroscopy (PCS) has evolved as an important technique for examining structural relaxation in amorphous polymers near the glass transition.³ PCS experiments probe relaxations of spatial fluctuations (on the order of 10^{-5} cm) in the local dielectric tensor that occur in the time window ranging from 10^{-6} to 10^2 s. In this experiment, the time scale for structural relaxation in bulk polymers can be controlled by varying temperature or pressure. Despite differences in primary chemical structure, the shape of the observed nonexponential decay in structural relaxation is relatively universal and depends only weakly on molecular weight.⁴

While the temperature dependence of the characteristic time for structural relaxation probed by PCS for bulk polymers near the glass–rubber transition is well described by the Williams–Landel–Ferry relation,¹ the

pressure dependence is not as well documented. Isolation of the effect of free volume (or density) on polymer dynamics from the effect of molecular internal energy on polymer dynamics can be achieved by using pressure as the primary variable for manipulating the relaxation time scale. To study backbone segmental dynamics near the glass transition, structural relaxation should be controlled by cooperative segmental dynamics and not by the motions of large pendant groups. An ideal material for such studies is poly(propylene oxide) (PPO). This polymer is amorphous and contains no bulky side groups whose relaxation dynamics would interfere with PCS measurements at temperatures above T_g (~ 200 K). This work addresses the dynamical behavior of amorphous polymers at high pressures as studied by PCS and extends the documented pressure range of structural relaxation studies.

The pressure dependence for the segmental relaxations in several glass-forming polymers has been studied by a variety of techniques including PCS, dielectric relaxation, and fluorescence decay, and all of these studies found similar pressure-dependent relaxation behavior. In dielectric relaxation studies⁵ of PPO, the dipole moment relaxation time increased exponentially with pressure over the range from 1 to 2800 bar. To date, all pressure studies using PCS^{6–8} have focused on acrylate polymers with glass transition temperatures near ambient conditions. Structural relaxation in these polymers is influenced by pendant group as well as main-chain motion at the experimental conditions probed by PCS. In these PCS measurements, the mean relaxation time increased exponentially with pressure from 1 to 2100 bars.

In this study, we present PCS measurements on low molecular weight PPO (MW = 4000) in the pressure range from 2.5 to 3.9 kbar. Consistent with a recent temperature study^{9,10} of PPO dynamics by PCS, the structural relaxation exhibits two distinct processes. The primary and stronger process is attributed to segmental reorientation while the secondary or weaker process is attributed to overall chain motion. Two relaxation processes have also been observed in dielectric studies^{11–13} of PPO samples with similar molecular weight, but only one relaxation process was reported in earlier PCS measurements.⁴ Based on our experiments, the mean relaxation time of the primary relaxation mode exhibits an exponential dependence on pressure with an activation volume of $92 \text{ cm}^3/\text{g}\cdot\text{mol}$ at

* Corresponding author.

[†] Current address: E. I. Dupont, Box 800, Kinston NC 28502.

[®] Abstract published in *Advance ACS Abstracts*, March 1, 1997.

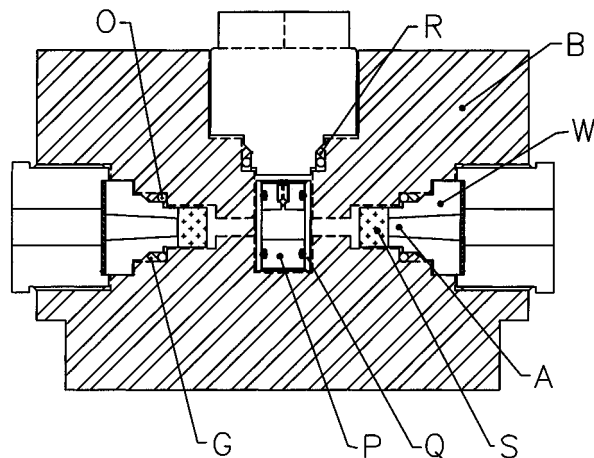


Figure 1. High-pressure optical cell: (A) window aperture; (B) cell body; (G) metal gasket (wedge-ring type); (O) Viton O-ring; (P) aluminum pistons; (Q) quartz sample cell; (R) metal gasket for sample port (SS304); (S) sapphire window; (W) window support. Windows at 45, 90, and 135° are omitted for clarity.

253 K. This volume is consistent with the value determined from dielectric studies⁵ (98 cm³/g·mol) at the same temperature.

Experimental Section

Photon correlation spectra of poly(propylene oxide) (MW = 4000, T_g of 200 K¹⁴) were recorded over a range of pressures (2.5–3.9 kbar) at a temperature of 253 K and a scattering angle of 90°. Fixing the temperature at 253 K moved the time scale for structural relaxation into the PCS experimental time window for pressures greater than 2 kbar. For pressures lower than 2 kbar, no structural relaxation was detected in the PCS time window. Temperature control was provided by a Lauda temperature bath which gave a temperature stability of ± 0.2 K. The light source was an argon ion laser (Coherent Innova 70-3) operating in intensity control mode at 514 nm with an output power of ~ 1 W. The VV-scattering spectrum was measured through a band-pass filter (514.5 nm) and a 200- μ m pinhole with a photomultiplier tube (BI-PMT 9836 from Brookhaven Instruments of Holtsville, NY). The correlator (BI-9000 from Brookhaven Instruments) employed logarithmic channel spacing, permitting correlation function sampling over eight decades in time. Logarithmic correlators eliminate the need for composite correlation functions generated from incremental sample times.

Sample measurements were performed using a high-pressure optical cell shown schematically in Figure 1. The cell was designed to operate at pressures up to 4 kbar and was constructed to fit atop a BI-200SM goniometer (Brookhaven Instruments) without modification. A similar design¹⁵ has been tested to 8 kbar. The high-pressure cell (height 9.4 cm, diameter 13.6 cm) was constructed from alloy tool steel (H13) and heat treated (HRC 45) for strength. The cylindrical cell body (B) has an axial hole (diameter 16 mm) which holds a quartz sample cell (Q). Three windows located at 45, 90, and 135° relative to the incident beam can be used for scattering measurements while windows at 0 and 180° served as the entrance and exit windows for the light source. Each angular port was fitted with a sapphire window (S) (length 8 mm, diameter 11 mm; Hemex quality) from Crystal Systems of Salem, MA. The window aperture was ~ 5 mm in diameter. In this geometry, the optical axis of the sapphire (0001) was coincident with the direction of the incident and scattered light. The sapphire windows were attached with Super Glue to an optically flat window support constructed in two pieces from heat-treated stainless steel (SS416).

The pressure-transmitting fluid (toluene) was supplied to the cell through a standard cone-and-thread connection from a hand-cranked pressure generator (Model 37.5-5.75-60 from High Pressure Equipment Co.). Since the experiments were

performed at subzero temperatures, water was removed from the toluene by contacting with molecular sieves (Sigma M-2635). Pressure was measured with a transducer (Dynisco Model G810-300-60M) with an accuracy of ± 10 bar. Temperature was measured with a resistive temperature device located in close proximity (~ 2 cm) to the sample cell. The upper section of the cell was covered by a heat exchanger connected to the temperature bath, and the entire cell was insulated.

Window and sample ports were sealed with a modified¹⁶ wedge-ring gasket. This self-energizing gasket (G) has a trapezoidal cross section in order to maximize the total unsupported area and was constructed from copper alloy (C52100). A stainless steel gasket was used for the sample port (instead of copper) because the copper alloy was easily extruded from this port, which has a larger unsupported area than the window ports. A supplemental Viton O-ring (O) provided an effective seal until gasket deformation could occur at ~ 2.2 kbar. The copper alloy gaskets proved durable and could be repeatedly pressurized so long as the window plug was not removed. This sample cell design isolates the pressurization mechanics from the difficulties of preparing clean, dust-free samples. Furthermore, the use of thin-wall quartz maintains a highly transparent optical path for these low-intensity scattering experiments.

The PPO sample (purchased from Aldrich Chemical) was dried in a vacuum oven over night at 70 °C and hot filtered through a 0.22- μ m filter (Millipore GVWP-025) directly into a dust-free sample cell constructed from optical-quality quartz (Suprasil). To contain and pressurize the liquid sample, a cylindrical quartz cell (length 25 mm, inside diameter 12 mm, outside diameter 15 mm) was fitted with aluminum pistons (P) and Viton O-rings on each end. After loading, the sample cell was surrounded by a dust-free index matching fluid (toluene) which also transmits pressure to the polymer sample through piston displacement. With this design, the possibility of sample contamination by the pressurizing fluid must be considered. Therefore, PCS measurements were repeated at 2.8 kbar after cycling the pressure to 4.2 kbar. The measured relaxation spectra were the same before and after cycling.

Data Analysis

The homodyne intensity autocorrelation function (IACF), $C(\mathbf{q}, \tau)$, measured with a photocathode is related to the dielectric fluctuation autocorrelation function $g^{(1)}(\mathbf{q}, t)$ by¹⁷

$$C(\mathbf{q}, t) = A(1 + b|g^{(1)}(\mathbf{q}, t)|^2) \quad (1)$$

where A is the baseline, b is the contrast factor which is determined experimentally, and \mathbf{q} is the scattering vector. Since dielectric fluctuations are most strongly coupled to local density fluctuations,¹⁷ $g^{(1)}(\mathbf{q}, t)$ can be described by the normalized density-fluctuation autocorrelation function given by

$$g^{(1)}(\mathbf{q}, t) = \frac{\langle \delta\rho(\mathbf{q}, t)\delta\rho(\mathbf{q}, 0) \rangle}{\langle |\delta\rho(\mathbf{q}, 0)|^2 \rangle} \quad (2)$$

where $\delta\rho(\mathbf{q}, t) = \rho(\mathbf{q}, t) - \langle \rho \rangle$ is the Fourier transform of local density fluctuation away from equilibrium and $\langle \rangle$ represents the ensemble or time average.¹⁷

Due to the complicated nature of molecular motions in bulk polymers, no fundamentally based expression for the nonexponential decay of the density fluctuation autocorrelation function and, therefore, the IACF is currently available. The measured autocorrelation function is usually well described by the empirical Kohlrausch–Williams–Watt (KWW) expression¹⁸ given by

$$g^{(1)}(t) = \exp[-(t/\tau_0)^\beta] \quad (3)$$

Table 1. Pressure Dependence of the Mean Relaxation Time, $\bar{\tau}$, and Relaxation Time Distribution, β , from the Intensity Autocorrelation Function of Poly(propylene oxide) (MW = 4000) at 253 K

P (kbar)	β	$\bar{\tau}$ (ms)	P (kbar)	β	$\bar{\tau}$ (ms)
2.5	0.30	2.4	3.3	0.35	65
2.8	0.31	8.0	3.6	0.37	250
3.0	0.33	20	3.9	0.39	980

where β ($0 < \beta \leq 1$) is a measure of the width of the distribution of relaxation times and τ_0 is the primary relaxation time. The mean relaxation time, $\bar{\tau}$, is calculated from

$$\bar{\tau} \equiv \int_0^\infty \exp[-(t/\tau_0)^\beta] dt = \frac{\tau_0}{\beta} \Gamma\left(\frac{1}{\beta}\right) \quad (4)$$

where Γ is the gamma function.

The parameters A and b that appear in eq 1 were determined experimentally. The parameter A is the measured baseline, determined by averaging the count rate from four correlator channels whose delay time exceeds the final correlation time by at least a factor of 4. Fits to eqs 1 and 3 were performed for $C(t)/A - 1 > 0.01$ – 0.02 , treating b as a fitting parameter only for the highest pressure, where the short-time plateau is obvious. This value of b was then fixed, and the best fit for τ_0 and β was determined for the remaining pressures. Alternatively, fitting b at each pressure yielded consistent values ($b \approx 0.29$) over the range of pressures studied. Results for the KWW parameters are summarized in Table 1. Fits of eq 3 to the experimental data are shown as solid curves in Figure 2. Typical uncertainty in the fit for β is ± 0.02 , and the uncertainty in the mean relaxation time, $\bar{\tau}$, is $\sim \pm 10\%$.

The IACF may also be inverted by Laplace transform techniques, such as Provencher's¹⁹ constrained regularization method, to obtain the weighted distribution of relaxation times without prior assumptions regarding the shape of the relaxation function. As in the case of mechanical relaxation experiments, the nonexponential decay for the correlation function is represented by a distribution of relaxation times²⁰ as

$$g^{(1)}(t) = \int_{-\infty}^{\infty} \exp(-(t/\tau)L(\ln \tau)) d \ln \tau \quad (5)$$

where $L(\ln \tau)$ represents the strength of the relaxation process at time τ .

Discussion

A. Multiple Relaxation Processes. Figure 2 presents the IACF versus time on a semilogarithmic scale for pressures ranging from 2.5 to 3.9 kbar at 253 K. The relaxation time increases as pressure increases. In addition to the primary relaxation at short times, we observe a distinct long-time correlation in the IACF decay (see, for example, the tail for $t > 10^{-1}$ at 3.9 kbar). A recent PCS study of the temperature dependence of density fluctuation relaxations in PPO-4000^{9,10} also reports similar long-time tails which were attributed to overall chain motion. A similar slow, so-called α' , process in dielectric studies of PPO-4000^{11–13} has been attributed to normal-mode relaxations. Since the polymerization of PPO proceeds almost completely by head-to-tail monomer additions, PPO belongs to a class of polymers that bear a cumulative dipole moment in the direction of the end-to-end vector.¹¹ Therefore, the relaxation of the end-to-end vector appears as a second-

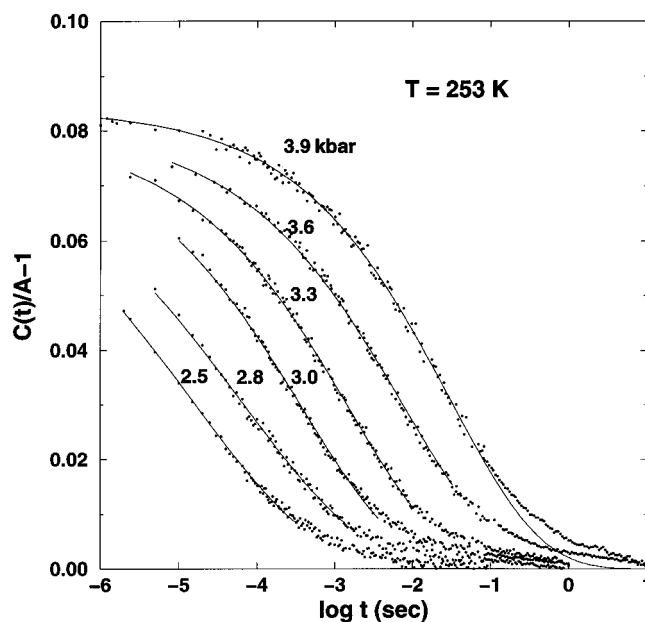


Figure 2. Normalized intensity autocorrelation function versus time at various pressures as indicated by the labels. Solid curves represent the best fit of eq 3 to the fast relaxation part of the curves ($C(t)/A - 1 > 0.01$). For $P = 3.9$ kbar, the KWW fit is extended to the base line to make the long-time tail more evident.

ary dispersion in the loss component of the dielectric relaxation.¹¹ Our results are consistent with dielectric and PCS temperature studies where the relaxation time for the long-time correlation is much greater than the characteristic time of the primary relaxation associated with cooperative segmental motions.

In samples near the glass transition, multiple relaxations in the PCS time window have been noted for several polymers including poly(methyl methacrylate),^{21,22} poly(ethyl methacrylate),⁷ poly(*n*-butyl methacrylate),⁸ and poly(methyl phenylsiloxane)²³ (PMPS). For the poly(acrylates), the fast relaxation process is attributed to the so-called β process associated with the localized motion of a polymer segment within a virtual cage formed by surrounding segments (e.g., pendant group motion). On the time scale of the β process, the cage appears frozen while at longer times the cooperative motions of surrounding molecules relax the cage, permitting segmental reorientation. This second, slower process of cage relaxation and cooperative segmental reorientation is associated with the α relaxation or glass transition. Since the pendant side groups are large for the acrylate samples, the strength of the β relaxation on the time scale probed by PCS is large and, therefore, detectable in a PCS experiment. Both processes are described by a KWW function but values for the stretching exponents (β) are not given.⁷ However, in a recent PPO study⁹ and a PMPS study,²³ the fast relaxation is ascribed to cooperative segmental dynamics and the slower relaxation to normal-mode processes. An obvious difference between the acrylate samples and the PPO/PMPS samples is polymer molecular weight, which is high for the acrylate samples (10^6 – 10^7) and low for the PPO and PMPS (MW = 27 000) samples. Also, the PMPS and PPO samples are liquids at room temperature while the acrylates are solids with T_g 's at or above room temperature. While structural relaxations due to cooperative segmental dynamics are not complicated by the motions of large pendant groups in PPO, the presence of normal-mode relaxations in the PCS time window does complicate spectral interpretation.

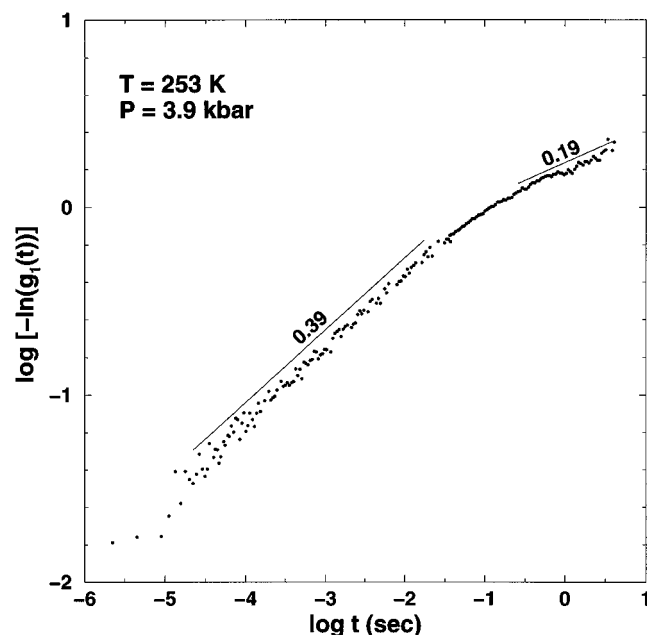


Figure 3. Renormalized ($b = 0.29$) density fluctuation auto-correlation function, $g^{(1)}(t)$, versus time at 3.9 kbar plotted in KWW form. Solid lines represent linear regression fits; these are labeled with their slopes and are shifted for clarity.

The parameters β and $\bar{\tau}$ determined from experimental data in Figure 2 are summarized in Table 1. Due to the presence of the long-time tail, curve-fitting procedures for the fast process were restricted to regions in which $C(t)/A - 1 > 0.01-0.02$. As pressure increases from 2.5 kbar to 3.9, the distribution of relaxation times narrows as indicated by an increase in β from 0.30 to 0.39. The value of β at the highest pressure (3.9 kbar) is consistent with the value obtained in ambient pressure studies^{4,9} of PPO dynamics. The increase in the stretching exponent, β , with increasing pressure is consistent with the notion that some relaxation modes become inaccessible on the time scale of the experiment as polymer free volume decreases and longer range segmental motions become frozen. Alternatively, values of β determined at lower pressures may also be overly influenced by the long-time relaxation process which has a broader relaxation time distribution than the faster relaxation process.

Figure 3 presents the normalized density fluctuation ACF, $g^{(1)}(t)$, at the highest pressure plotted in a double-logarithmic form (according to eq 3) to illustrate the two distinct exponents for the short- and long-time relaxations. We observe a smooth transition, centered around 0.1 s, from a slope of 0.39–0.19. The stretching exponent for the long-time process (0.19 ± 0.05) agrees with the value of 0.2 ± 0.05 found in a recent temperature study⁹ of PPO dynamics by PCS. Interestingly, in that study, stretching exponents from the long- and short-time relaxations compared favorably with predictions of the mode-coupling theory.²⁴

Figure 4 presents the distribution of relaxation times extracted from the normalized IACF as a function of time at 3.3 and 3.9 kbar. The analysis was performed using the CONTIN program,¹⁹ which applies a numerical inverse Laplace transform to extract a relaxation time distribution without prior assumptions about the functional form of the structural relaxation. The resulting curves exhibit two distinct peaks separated by almost 3 orders of magnitude in time. Short-time shoulders appear on the edge of the relaxation peaks

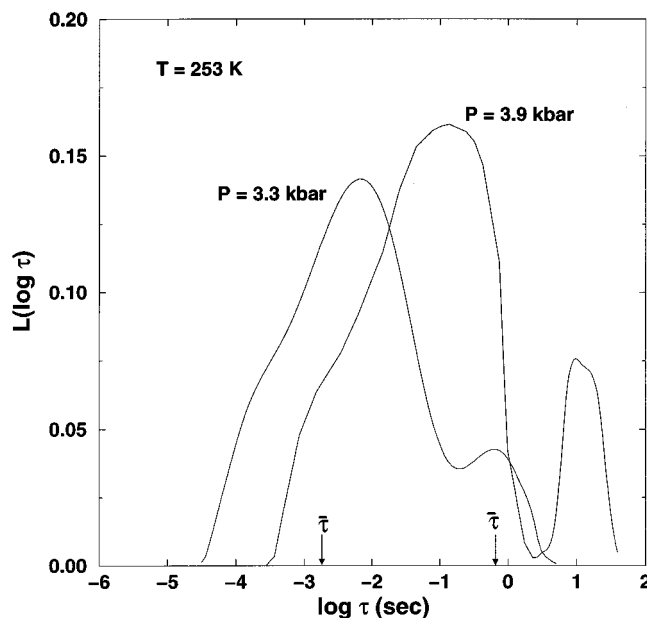


Figure 4. Relaxation time distributions extracted with the inverse Laplace transformation technique for PPO-4000 at 253 K and 3.3 and 3.9 kbar. The two-peak structure indicates the presence of two distinct relaxation processes. The mean relaxation times determined by fitting experimental results to the KWW model, $\bar{\tau}$, are indicated by the arrows.

associated with the faster process. It is not known whether the short-time shoulder is an artifact of the inversion technique or a reflection of the structural relaxation process. These results appear very similar to the relaxation time distribution for PMPS (see Figure 5 of ref 23). Dielectric studies^{11–13} of PPO samples of similar molecular weight also report a strong dispersion (α' process) ascribed to normal-mode relaxation of chain subsections. In these dielectric studies, the primary and secondary relaxation times in PPO are also separated by ~ 3 orders in magnitude. While PCS studies have not definitively shown Rouse-mode relaxation in a single component fluid, the observed relaxation time of the slow process (~ 1 s) is consistent with the normal-mode relaxation time for a Rouse chain in a high-friction environment.²⁵

B. Activation Volume. Structural relaxation times for polymeric materials typically increase exponentially with pressure.^{5–26} Figure 5 illustrates the large effect of pressure on the mean relaxation time, $\bar{\tau}$, since the IACF decay shifts to longer times as pressure increases. Assuming that the faster relaxation (α -process) is an activated process, the activation volume can be determined from transition state theory. The activation volume is related to the pressure-dependent relaxation time by

$$\Delta V^\ddagger = (\partial \ln \tau / \partial P)_T RT \quad (6)$$

where ΔV^\ddagger is the difference between the equilibrium molar volume and the volume required for a transition to a new conformation, R is the gas constant (83.144 cm³ bar/g mol K), and T is the absolute temperature. Figure 5 shows a linear dependence of $\ln \bar{\tau}$ on pressure at 253 K over the range of pressures studied. The activation volume determined from the slope of the solid line in Figure 5 is 92 ± 3 cm³/g·mol at 253 K, which is only slightly smaller than the volume (98 cm³/g·mol) determined from pressure studies⁵ of dielectric relaxation in high molecular weight PPO ($\sim 10^6$) at the same

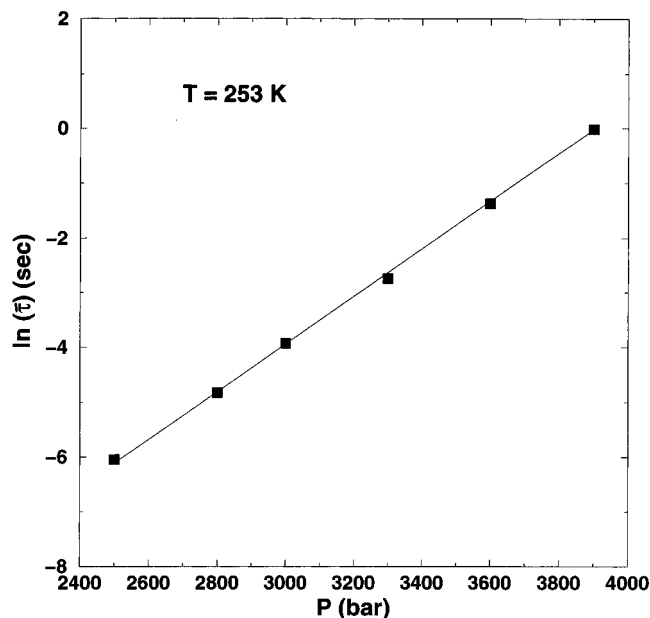


Figure 5. Pressure dependence of the mean relaxation time for PPO-4000 at 253 K.

temperature. Given the higher concentration of end groups in our relatively low molecular weight PPO, a lower activation volume is not surprising. Since the molar volume of a repeat unit in PPO is $58 \text{ cm}^3/\text{g}\cdot\text{mol}$,²⁶ the measured activation volume is approximately twice the size of a repeat unit for the α relaxation process probed by PCS at this temperature.

In mechanical studies of polymer relaxation,^{27,28} the logarithm of the relaxation time is often linearly dependent upon the applied hydrostatic pressure. The pressure dependence can be described as

$$\ln \frac{\tau(P)}{\tau(P_0)} \equiv \ln a_p = \theta(P - P_0) \quad (7)$$

where a_p is the shift factor relative to a reference pressure P_0 and θ equals $\Delta V^\ddagger/RT$ from eq 6. Figure 6 presents a master curve of all the IACFs constructed from time shifts (performed graphically) of the individual IACFs using a reference pressure of 3.3 kbar. The inset shows the dependence of a_p on pressure, and the solid line is a fit to eq 7. Some deviations in the master curve construction are observed in the short-time region, but the superposition is relatively good and yields a decay covering almost 9 decades in time. The better registry of the dynamic relaxation at long times is consistent with superposition techniques applied in mechanical experiments, which generally probe long-time dynamics. Some deviations at short times were also noted in the PMPS study (See Figure 4b of ref 23). The relatively good registry of the shifted IACF over a 1.5-kbar range indicates the applicability of the time-pressure superposition principle.¹ A KWW fit to the entire master curve (solid line in Figure 6) yields $\beta = 0.35$ and $\bar{\tau} = 57 \text{ ms}$. Since the fit is not weighted and the number of data points at short times is low, the best fit ($b = 0.30$) overshoots the initial decay in order to minimize the error at longer times. The pressure dependence of the shift factor (See inset in Figure 6) provides a second estimate of the activation volume. A linear regression analysis yields a value of $98 \text{ cm}^3/\text{g}\cdot\text{mol}$, which is consistent with the value of $92 \text{ cm}^3/\text{g}\cdot\text{mol}$ obtained from our fits to the KWW function.

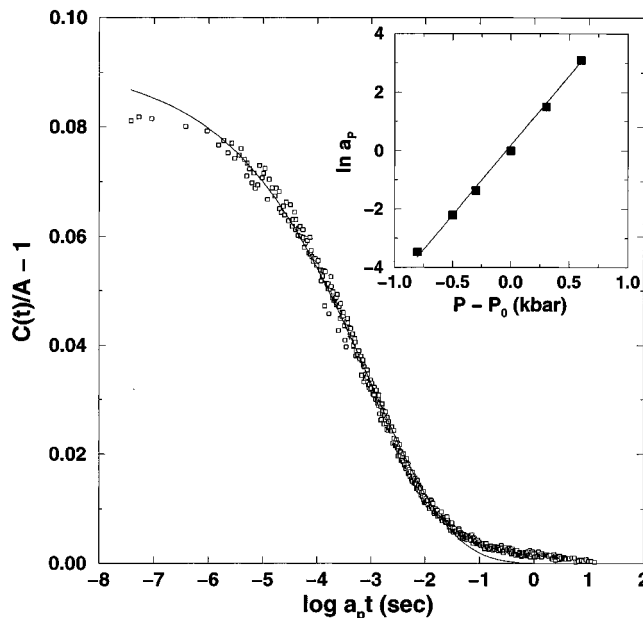


Figure 6. Master curve of the IACFs constructed graphically from shifts of the individual IACFs using a reference pressure, P_0 , of 3.3 kbar. A best fit of the KWW equation to the entire curve is also shown and does not adequately describe the long-time process. The inset shows the dependence of the shift factor, a_p , on pressure.

Summary

We have presented a photon correlation study in which pressures ranging from 2.5 to 3.9 kbar are used to probe the effect of pressure on the structural relaxation of poly(propylene) oxide. In addition to segmental relaxations, which are well described by a stretched exponential fit, a slower relaxation mode is observed. This slow, broad relaxation is ascribed to normal-mode processes in the relatively low molecular weight sample. The pressure-dependent relaxation time for the fast relaxation process provides an estimate for the activation volume that is consistent with determinations from dielectric relaxation studies. The stretching exponent for the long-time process at the highest pressure agrees well with a recent temperature study of PPO dynamics.⁹

Acknowledgment. This work was supported in part by the National Science Foundation (Young Investigator Award CTS-9257911 (B.D.F.)) and by the Director, Office of Basic Sciences, Chemical Sciences Division of the U.S. Department of Energy under Contract DE-FG05-91ER1418 (C.K.H.). The authors gratefully acknowledge discussions with Dr. Philippe Sergot (École Supérieure de Physique et de Chimie Industrielles de la Ville de Paris) concerning the quartz sample cell design and J. Emerick (Precision Engineering Machine Shop, NCSU) for optical cell construction.

References and Notes

- (1) Ferry, J. D. *Viscoelastic Properties of Polymers*; Wiley: New York, 1980.
- (2) Duggal, A. R.; Nelson, K. A. *J. Chem. Phys.*, **1991**, *94*, 7677.
- (3) Pecora, R. *Dynamic Light Scattering. Applications of Photon Correlation Spectroscopy*; Plenum: New York, 1985.
- (4) Wang, C. H.; Fytas, G.; Lilge, D.; Dorfmueller, T. *Macromolecules* **1981**, *14*, 1363.
- (5) Williams, G. *Trans. Farad. Soc.*, **1965**, *61*, 1564.
- (6) Fytas, G.; Patkowski, A.; Meier, G.; Dorfmueller, T. *Macromolecules* **1982**, *15*, 870.
- (7) Fytas, G.; Patkowski, A.; Meier, G.; Dorfmueller, T. *J. Chem. Phys.*, **1984**, *80*, 2214.
- (8) Meier, G.; Fytas, G.; Dorfmueller, T. *Macromolecules* **1984**, *17*, 957.

- (9) Sidebottom, D. L.; Bergman, R.; Börjesson, L.; Torrell, L. M. *Phys. Rev. Lett.*, **1992**, 68, 3587.
- (10) Sidebottom, D. L.; Bergman, R.; Börjesson, L.; Torrell, L. M. *Prog. Colloid Polym. Sci.*, **1993**, 91, 43.
- (11) Baur, M. E.; Stockmayer, W. H. *J. Chem. Phys.*, **1965**, 43, 4319.
- (12) Alper, T.; Barlow, J.; Gray, R. W.; *Polymer*, **1976**, 17, 665.
- (13) Johari, G. P.; *Polymer*, **1986**, 27, 867.
- (14) Johari, G. P.; Hallbrucker, A.; Mayer, E. *J. Poly. Sci. Part B: Poly. Phys.*, **1988**, 26, 1923.
- (15) Hara, K.; Morishima, I. *Rev. Sci. Instrum.*, **1988**, 59, 2397.
- (16) Whalley, E.; Lavergne, A.; Wong, P. T. T. *Rev. Sci. Instrum.*, **1976**, 47, 845.
- (17) Berne, B. J.; Pecora, R. *Dynamic Light Scattering*, Kreiger: Malabar, FL, 1990.
- (18) Williams, G.; Watts, D. C. *NMR Basic Princ. Prog.* **1971**, 4, 271.
- (19) Provencher, S. W. *Comput. Phys. Commun.*, **1982**, 27, 213, 229.
- (20) Hagenah, J.-U.; Meier, G.; Fytas, G.; Fischer, E. W. *Polym. J.* **1987**, 19, 441.
- (21) Fytas, G.; Wang, C. H.; Fischer, E. W.; Mehler, K. *J. Poly. Sci. Part B: Poly. Phys.*, **1986**, 24, 1859.
- (22) Fytas, G.; Wang, C. H.; Fischer, E. W. *Macromolecules* **1988**, 21, 2253.
- (23) Boese, D.; Momper, B.; Meier, G.; Kremer, F.; Hagenah, J. U.; Fischer, E. W. *Macromolecules* **1989**, 22, 4416.
- (24) Fuchs, M.; Götzl, W.; Latz, A. *J. Phys. Condens. Matt.* **1991**, 3, 5047.
- (25) Rouse, P. E. *J. Chem. Phys.* **1953**, 21, 1272.
- (26) Freeman, B. D.; Bokobza, L.; Sergot, P.; Monnerie, L.; DeSchryver, F. C. *Macromolecules* **1990**, 23, 2566.
- (27) Ferry, J. D.; Stratton, R. A. *Kolloid-Z.* **1960**, 171, 107.

MA960408+